MECHANISMS OF ZEBRA STRUCTURE GENERATION IN SOLAR RADIO EMISSION AGAINST THE BACKGROUND OF COMPLEX DYNAMIC SPECTRA

G.P. Chernov*, V.V. Fomichev**

Pushkov Institute of Terrestrial Magnetism, Ionosphere and Radio Wave Propagation of the Russian Academy of Sciences (IZMIRAN), Moscow, Troitsk, Russia

** e-mail: gchernov @ izmiran . ru*

***e-mail: fomichev @ izmiran . ru*

Received February, 29 2024

Revised May, 01 2024

Accepted for publication July, 25 2024

The discussion about the origin of zebra structure has been continuing for more than 50 years. In many works, it is usually postulated that the double plasma resonance mechanism always works if there are fast particles in a magnetic trap. Due to a number of difficulties encountered by this mechanism, works on its improvement began to appear, mainly in a dozen articles by Karlicky and Yasnov, where all discussion is based on the variability of the ratio of scales of magnetic field and density variations and the assumption of some plasma turbulence in the source. Here we show the possibilities of an alternative model of interaction of plasma waves with whistlers. Several phenomena were selected in which it is clear that the ratio of variation scales does not change in the magnetic loop as a source of zebra structure. It was shown that all the main details of the sporadic zebra structure in the event of August 1, 2010 (and in many other events) can be explained within a unified model of zebra structure and fiber bursts during the interaction of plasma waves with whistlers. The main changes in the zebra structure bands are caused by the scattering of fast particles on whistlers, leading to the switching of whistler instability from the normal Doppler effect to the anomalous one. Finally, the possibilities of laboratory experiments are considered, and the solar zebra structure is compared with similar bands in the decameter radio emission of Jupiter.

DOI: 10.31857/S00167940250102e1

1. INTRODUCTION

Understanding the nature of fine structure in solar radio burst emission is one of the most important criteria for verifying radio emission mechanisms. Zebra pattern (ZP) belongs to the most remarkable type of fine structure. On dynamic spectra, it appears as regular stripes in emission and absorption. It has been described in numerous articles and monographs, starting from the first publication by Elgar ø y [1959; Kuijpers, 1975; Slottje, 1981; Chernov, 1976; 2006; 2011].

The discussion about the origin of zebra pattern has continued for more than 50 years [Chernov, 2011]. Most often, the mechanism based on double plasma resonance (DPR) is discussed [Zheleznykov and Zlotnik, 1975a, b]:

$$\omega_{UH} = (\omega^2_{Pe} + \omega^2_{Be})^{1/2} = s\,\omega_{Be}, \qquad (1)$$

where ω_{Pe} − electron plasma frequency, ω_{Be} − electron gyrofrequency under conditions when $\omega_{Be} \ll \omega_{Pe}$ [Zheleznykov and Zlotnik, 1975a , b; Kuijpers, 1975; 1980; Mollwo, 1983; 1988; Winglee and Dulk, 1986]. In these works, it is usually postulated that the mechanism always operates if there are fast particles in the magnetic trap. However, it faces a number of difficulties in explaining the dynamics of ZP stripes (sharp changes in frequency drift of the stripes, large number of harmonics, frequency splitting of stripes, their superfine structure in the form of millisecond spikes). Therefore, works began to appear both on its improvement [Karlický et al., 2001 ; LaBelle et al., 2003; Kuznetsov and Tsap, 2007], and related to the creation of new models.

In a dozen works by Karlický and Yasnov, within the DPR framework, the method for estimating the number of harmonics was improved, mainly toward increasing it, bringing it up to 170-200. At the same time, comparisons with other models were usually not made.

Here we note some of their important results with their discussion in the framework of an alternative whistler-based zebra model.

2. COMPLEX SPECTRA OF ZEBRA-STRUCTURE

Figure 1 and Figure 2 show spectra of zebra structure with different parameters of stripes both over time and at different frequencies. Here it is difficult to justify the application of the DPR mechanism even for individual sections of the spectrum, ignoring the rest.

Fig. 1.

Fig. 2.

Almost simultaneously with the DPR, an alternative mechanism of interaction between plasma waves (l) and whistlers (w), $l + w \rightarrow t$ was proposed [Chernov, 1976; 1990]. In this model, the fine effects of ZS bands listed above are explained by quasi-linear effects of the interaction of fast particles with whistlers. The whistler mechanism became its natural development after its application by Kuijpers [Kuijpers, 1975] for fiber bursts, when in some phenomena a continuous transition of ZS bands into fibers and back was observed. The most important details of this mechanism are presented in the Discussion section.

In the fundamental work on the DPR mechanism [Zheleznykov and Zlotnik, 1975a], it was shown that the relative bandwidth of the increment in the hybrid band is incredibly narrow $\delta\omega/\omega_{Be}$ ~$2.5\cdot10^{-4}$. Such a value is obtained only under the condition that the velocity dispersion of the particle beam is generally discarded as an infinitesimal value in the estimates. In [Benáček et al., 2017], it is shown that accounting for the velocity dispersion of hot particles and the temperature of cold plasma severely limits the effectiveness of the DPR mechanism. Then Karlický and Yasnov made a significant contribution to improving the DPR mechanism in a dozen of their works. In one of their recent papers [Yasnov and Karlický, 2020], they made an important update to this activity. After the article [Yasnov and Chernov, 2020], they pointed out the importance of considering changes in the ratio of scales of magnetic field and density variations in the source of the zebra structure when analyzing any phenomenon. For example, in [Yasnov and Chernov, 2020], this ratio was considered constant, and the advantage of the whistler mechanism for the event of 06.21.2011 was demonstrated.

In the introduction of [Yasnov and Karlický, 2020], the authors noted all the major works on observations of zebra structure and theoretical mechanisms for its explanation (more than 20 articles), which relieves us from the necessity to repeat them here. They proposed an improved method for determining the gyroharmonic of zebra stripes, which is essential for determining the electron density and magnetic field strength in the zebra source. In comparison with previous methods, a new assumption was made that the ratio $R = L_{bh} / L_{nh}$ (where L_{bh} and L_{nh} − are characteristic scales of magnetic field and density variations) changes in the source in a more generalized form. Almost free manipulation of the variability of R allows to obtain new values of gyrofrequency numbers around 115 for the event of 06.21.2011 (instead of 50 – 60 in the work Yasnov and Chernov, 2020], and up to 170 in other events. At the same time, the previous results of the authors [Benáček et al., 2017] are not mentioned, where it was shown that in real parameters, the increment amplitude of the cone instability significantly decreases by the 30th harmonic.

This fact alone indicates the unsuitability of the proposed improvement of the DPR model, in particular, for determining the harmonic number of zebra structure stripes by manipulating the inconsistency of the ratio of scales of magnetic field and density changes both in a single event and in different ones.

In the previous work [Karlický, 2014], it was assumed that all frequency variations of zebra stripes are caused by some turbulence. In recent articles, everything is connected with the propagation of a fast magnetosonic wave [Karlický, 2022], as a strict period of fluctuations was determined there, coinciding with the classical cosine function. Interestingly, the phenomenon of August 17, 1998 is being analyzed once again, after the first consideration in the work [Zlonik et al., 2009]. These are rapid pulsations of zebra structure packets (similar to type III bursts) against the background of pulsations in absorption. [Zlonik et al., 2009] believed that two non-equilibrium distribution functions were present in the source: one with a conical velocity distribution, responsible for continuum radiation, and another of the Dory, Guest, and Harris type, capable of causing the DPR effect, producing zebra structure. [Karlický, 2022] does not mention this. The operation of the DPR mechanism is assumed, and the harmonic number at the lower frequency is determined by a newly developed method (mentioned above) for 13 zebra moments at different frequencies from 254 to 287 MHz. The maximum harmonic numbers were obtained at a frequency of 270.6 MHz, s 1= 177.6 and at 268.6 MHz s 1 = 214.6.

Such large improbable harmonics stimulate the reminder of an alternative interpretation of this phenomenon. In the review [Chernov, 2019], some properties of the spectrum with ZS packets are noted, which have not been considered anywhere since the work [Zlotnik et al., 2009]. Not all ZS packets have a negative frequency drift (like type III bursts). One can see a number of moments with positive drift. ZS is visible between packets, and continuous zebra bands can be seen throughout five packets with a noticeable sawtooth frequency drift. Between the ZS packets, pulsations in absorption have a diverse frequency drift.

Similar spectra with almost vertical zebra stripe packages have been observed in many events, starting with an excellent example in Fig. 6 in [Slottje, 1972]. In the event of July 3, 1974, similar zebra stripe packages appeared over several hours [Slottje, 1972; Chernov, 1976]. Previously, we have already shown the advantage of the whistler model for interpreting the event of 21.06.2011 [Yasnov and Chernov, 2020]. Even earlier, to explain the sawtooth frequency drift of zebra stripes in the well-known event of 25.10.1994, a mechanism with whistlers based on the scattering of fast particles on whistlers was applied [Chernov, 2005]. Whistlers are always generated simultaneously with plasma waves at the upper hybrid frequency by fast particles with a cone-shaped velocity distribution. The scattering process on whistlers was used in [Chernov, 1990] and in more detail in [Chernov, 1996; 2005]. There, an important property of the process was considered: the change in the direction of frequency drift of zebra stripes should correlate with the change in the direction of spatial drift of their radio emission sources (see Fig. 2 in [Chernov, 2019]).

During the scattering of fast particles on whistlers, the distribution function changes, and the generation of whistlers can repeatedly switch from the normal Doppler effect to the anomalous one. In [Zlotnik et al., 2003], for the event of 25.10.1994, the barometric formula is used to determine the temperature and select the magnetic loop. However, the concentration distribution according to the barometric formula cannot be applied in magnetic loops with plasma $\beta \ll 1$, since this formula gives the density distribution in a gravitational field at constant temperature and without taking into account the magnetic field.

During the scattering of fast particles on whistlers, the distribution function changes, and the generation of whistlers can repeatedly switch from the normal Doppler effect to the anomalous one (fan instability).

If fast particles interact with whistlers at cyclotron resonance

$$\omega^{w} - k_{\parallel} v_{\parallel} - s\,\omega_{Be} = 0 \qquad (2)$$

(at normal Doppler resonance $s = +1$), waves and particles are oppositely directed ($k_{\parallel} v_{\parallel} < 0$ or $\omega / k_{\parallel} < 0$) ($k_{\parallel}$ and $v_{\parallel}$ − components of the wave vector and velocity parallel to the magnetic field), particles move along diffusion curves. When the maximum of the distribution function shifts toward larger $v_{\parallel}$, the anomalous Doppler effect is activated ($s = -1$ in (1)). In these cases, the group velocity of whistlers reverses sign (smoothly or abruptly depending on the parameters of fast particles). And as a result, the frequency drift of the stripes synchronously reverses (see [Chernov, 1996] for details).

Karlicky and Yasnov usually analyze phenomena with regular zebra stripes, but more often the spectra are very complex with overlapping not only of fast pulsations, but with fibers (fiber bursts) with different frequency drifts, which are sometimes difficult to distinguish from ZS (for example, as in Fig. 1 and 2).

The entire discussion is based on the variability of the ratio of scales of magnetic field and density changes. This already indicates difficulties for the DPR model. From the spectra of a number of events, it becomes clear that the ratio of scales of field and density changes cannot change instantaneously in a loop.

Moreover, they use a number of known events with a large number of stripes, without addressing many other effects in the same spectrum. For example, ignoring explanations of the sawtooth frequency spectrum of the stripes, the connection with fast pulsations, sharp transitions, jumps in stripe parameters at the same frequencies, and other aspects.

3. DISCUSSION

The application of the DPR mechanism is simply postulated. After the extensive review [Zheleznyakov et al., 2016], there is no need to repeat its description in detail now. It remains the most cited mechanism in the analysis of zebra structure. It is based on the generation of plasma waves at the upper hybrid frequency ω_{UH} by fast electrons with a velocity distribution function having a loss-cone. Their subsequent transformation into electromagnetic waves creates continuum radiation, which can be sharply enhanced at DPR levels, where ω_{UH} is approximately equal to an integer number s of electron cyclotron harmonics ($\approx s\ \omega_{Be}$). This simple algebraic relationship forms the basis of the elegant theory of zebra structure (which has become almost classical), presented in the works [Zheleznyakov and Zlotnik, 1975a, b] and later supported in [Winglee and Dulk, 1986].

The main condition for the existence of many DPR levels suggests that the scale of magnetic field variation should be much smaller than the scale of density variation. However, this condition is shown in the listed works as a hypothetical scheme without numerical scales on the axes, shown in Fig. 3 *a* as a fragment of Fig. 2 in the review [Zheleznyakov et al., 2016] .

Fig. 3.

If we try to use for this the known analytical expressions for the dependence of density and magnetic field in the corona, then no known models confirm the possibility of forming many DPR levels within reasonable dimensions of zebra structure sources. For clarity, see Fig. 6 and 7 in the book [Chernov, 2019] on page 217, which raise doubts about using the DPR model to explain numerous zebra stripes, even without considering many effects of complex stripe dynamics.

Fig. 4.

Fig. 4 shows the calculation of DPR levels using normal (generally accepted) parameters of coronal plasma according to the barometric formula: electron temperature $Te = 1.2 \cdot 10^6$ K, initial plasma frequency f_{P0} = 3800 MHz at height h_{B0} = 20000 km. If a dipole dependence of the magnetic field is used for cyclotron harmonics, then harmonics with $s \geq 50$ move to much greater heights $\geq$ 100000 km. Thus, the excitation of waves simultaneously at 34 DPR levels in the corona is not feasible in any realistic models of density and magnetic field. In recent works, Karlicky and Yasnov proposed an exotic model (figure 3 *b*) with a hump on a smooth density decline [Selhorst et al., 2008], on the steep slopes of which DPR conditions should be met for the generation of a large number of harmonics Yasnov et al., 2016].

Fig. 1 shows a spectrum with a duration of about 45 s with a complex zebra structure, but in the absence of regular stripes, it is difficult to find a moment where the DPR mechanism could be applied. A broad absorption band intrudes into the zebra structure, against which a chain of narrow-band (rope-like) fibers develops [Chernov, 1997; 2008; Chernov et al., 2007].

In Fig. 2, the structure of the stripes changes dramatically in 15 s - fibers (similar to fiber bursts) smoothly transform into zebra stripes with a wave-like frequency drift. Obviously, the ratio of the scales of field and density variations cannot change noticeably within a few seconds.

Zebra spectra with sawtooth frequency drift of stripes were considered in the work [Karlický, 2014] on the example of spectra obs. Ondřejov in the decimeter range during the event of 08/01/2010. Without going into details, we note that the aim of the work was to show that within the DPR model, the zebra structure source is in a turbulent state based on the Fourier analysis of time intensity profiles of bands with frequency (and from the relations $\omega_{UH} \approx \omega_{Pe}$ and $n_e \sim \omega^2_{Pe}$ and with plasma density). The Fourier oscillation profile of density is taken as the calculated profile of the zebra band (apparently assuming that this does not require proof). The power spectrum of oscillations has a power-law form with an index of −5/3, coinciding with the Kolmogorov spectrum for turbulence.

Independently of this work, the article [Chernov et al., 2018] showed that all the main details of the sporadic zebra structure in the event of August 1, 2010, can be explained within the framework of a unified model of zebra structure and radio fibers during the interaction of plasma waves with whistlers (without strong plasma turbulence in the source). The main changes in the zebra structure bands are caused by the scattering of fast particles on whistlers, leading to the switching of whistler instability from the normal Doppler effect to the anomalous one.

3.1. Modeling of ZS bands

In connection with the above remark about the impossibility of obtaining many DPR levels in any known models of density and magnetic field (see Fig. 4), we can note the work [Karlický, 2022] on modeling solar radio zebra. In fact, this is not simulation, but fitting plasma parameters in the source to obtain model points on the zebra band in the spectrum that coincide with the observed ones, without calculating the generation of radiation within the DPR mechanism, simply plotting a graph like Figure 4 . Moreover, the main conclusion at the end confirms our conclusion (without reference), since the selected field values do not coincide with any known models. There is also a practical conclusion at the end: it is necessary to continue calculating the increments of upper hybrid waves for higher harmonic numbers (in the article s = 120–124).

In the spectrum of Fig. 2, at its beginning, a smooth transition of fiber bursts into zebra stripes with sawtooth frequency drift is visible. The same transition or reverse was observed in the event of August 1, 2010. Karlický [Karlický, 2014] does not discuss this effect, which is probably related to the fact that earlier in [Karlický, 2013] the model of fiber excitation on whistlers [Kuijpres, 1975] is rejected and a new or modified model [Treumann et al., 1990] based on Alfvén solitons is proposed.

3.2. Explosive instability

The mechanism proposed in [Fomichev et al., 2009] based on the stabilization of explosive instability during cascade growth of ion-sound harmonics, proves to be significantly more effective than the whistler instability mechanism on ion sound harmonics. It provides a large number of ZS harmonics with frequency separation independent of the ratio of plasma and cyclotron frequencies in the source and increasing with frequency (in accordance with observations). No additional strict conditions are imposed. The previous condition of acceleration of mono-velocity beams of weakly relativistic particles remains, which is usually realized in any major flare.

3.3. Laboratory experiments ([Viktorov et al., 2015])

Fig. 5.

To confirm the effectiveness of the DPR mechanism, sometimes reference is made to possibly the only work on creating radiation on DPR in a laboratory plasma experiment [Viktorov et al., 2015]. Although references to it are gradually fading [Chernov, 2019], since it demonstrates ambiguous results (according to Fig. 5): radiation is recorded only in the form of complex bands at the second harmonic of the cyclotron frequency, while the experiment also demonstrated the third harmonic (in Fig. 2). And if it were so simple to model, one could expect multiple repetitions of the experiment, which would indeed be proof of the mechanism's operation. However, there were only assurances from the authors that they were striving to obtain radiation at the third harmonic.

It is notable that Viktorov et al. [2015] show in their experiment simultaneous generation of whistlers at a frequency near $0.5 f_{ce}$ in Fig. 3b and a complex-shaped band near the frequency $2 f_{ce}$ in Figs. c and d, but the authors did not include these facts in the subject of their work.

3.4. Zebra pattern in the decameter radio emission of Jupiter ([Panchenko et al., 2018])

Fig. 6.

Observations of ZP, similar to that in solar radio emission, were conducted on the large ground-based radio telescope URAN-2 (Poltava, Ukraine) [Litvinenko et al., 2016]. The ZP bands (see Fig. 6) represent strongly polarized radio emission with durations from 20 to 290 s with a flux density of ~105 – 106 Jy (normalized to 1 AU), that is, 1 – 2 orders of magnitude lower than for the decameter radio emission of its moon Io. The frequency splitting between the bands increases slightly with increasing emission frequency (in 43 events), typically within the range of 0.5 – 1.5 MHz. In all examples, the bands exhibit rapid wave-like frequency drift while remaining quasi-equidistant from each other. All these facts are similar to the solar ZP.

Unlike the solar corona, Jupiter's plasma is highly anisotropic, i.e., $f_{pe} \ll f_{ce}$, in most regions of the magnetosphere. Therefore, the DPR mechanism with electrons cannot explain our observations, as this would require an extremely high plasma density, which is very unlikely in Jupiter's magnetosphere. [Zlotnik et al., 2016] proposed an alternative mechanism for the formation of zebra pattern in Jupiter's kilometer emission. The model is based on DPR on ion cyclotron harmonics. The mechanism involves the excitation of ion cyclotron waves at the lower hybrid frequency (f_{LH}), followed by nonlinear conversion of this low-frequency radiation into a high-frequency wave through a merging process with a high-frequency mode.

DPR with ions can operate in regions where $f_{pe} \ll f_{ce}$, which is fulfilled in most regions of Jupiter's magnetosphere. Therefore, the DPR effect on ion cyclotron harmonics can be realized at much lower plasma densities than the DPR effect on electron cyclotron harmonics. In this case, $f_{LH} \approx f_{pi}$ (f_{pi} is the ion plasma frequency), and the resonance condition is $f_{LH} = sf_{ci}$. Low-frequency plasma waves cannot leave the source and must first be converted into high-frequency electromagnetic waves (f_{em}) in the process of nonlinear merging with a high-frequency mode (for example, with plasma waves at the upper hybrid frequency). The merging of these waves ($f_{em} = sf_{ci} + f_{ce}$) leads to the generation of electromagnetic waves with a spectrum in the form of ZS. Nevertheless, additional theoretical studies are needed to clarify the nonlinear mode conversion from low-frequency ion cyclotron waves to high-frequency electromagnetic waves.

4. PRELIMINARY CONCLUSIONS

A brief review of possible alternative mechanisms for the excitation of zebra structure in connection with the difficulties of the DPR mechanism noted in the Introduction shows that possible models for the simultaneous excitation of many zebra bands can be the whistler mechanism and explosive instability (scattering of nonlinear ion-acoustic waves on particles). They do not require any additional conditions (or restrictions) on plasma parameters.

Radio sources of fiber bursts and ZS in the whistler model should have moving sources, and the spatial drift of ZS bands should change synchronously with the change in frequency drift on the dynamic spectrum. In the DPR model, the ZS source should be rather stationary.

There are more developed theories, but there is no final solution for them. For example, propagation through a medium with inhomogeneities assumes their presence with certain scales [Laptuhov and Chernov, 2006; 2009]. An even more detailed analysis of zebra in Jupiter's radio emission is required.

The global network of radio telescopes CALLISTO currently does not allow using its spectra, almost 90% of them are affected by local interferences, and the low frequency resolution of clean spectra does not allow registering zebra pattern stripes.

ACKNOWLEDGEMENTS

The authors are grateful to the RHESSI, GOES, LASCO spacecraft teams for open access to their data.

FUNDING

This work was supported by the Project of the Ministry of Education and Science KP19-270.

REFERENCES

- *Benáček J., Karlicky M., Yasnov L.V* . Temperature dependent growth rates of the upper-hybrid waves and solar radio zebra patterns // Astron. Astrophys. V. 598. ID A108. 2017. https://doi.org/10.1051/0004-6361/201629395
- *Chernov G.P.* Microstructure in the continuous radiation of type IV meter bursts. Modulation of continuous emission by wave packets of whistlers // Sov. Astron. V. 20. N 5. P. 582–589 . 1976.
- *Chernov G.P.* Whistlers in the solar corona and their relevance to fine structures of type IV radio emission // Sol. Phys. V. 130. N 1–2. P. 75–82. 1990. https://doi.org/10.1007/BF00156780
- *Chernov G.P.* A manifestation of quasilinear diffusion in whistlers in the fine structure of type IV solar radio bursts // Astron. Rep. V. 40. N 4. P. 561–568. 1996.
- *Chernov G.P.* The relationship between fine structure of the solar radio emission at meter wavelengths and coronal transients // Astron. Lett. V. 23. N 6. P. 827–837. 1997.

– *Chernov G.P.* Solar radio burst with drifting stripes in emission and absorption // Space Sci. Rev. V. 127. N 1–4. P. 195–326. 2006. https://doi.org/10.10007/s11214-006-9141-7
– *Chernov G.P., Stanislavsky A.A., Konovalenko A.A., Abranin E. P., Dorovsky V. V., Rucker H.O.* Fine structure of decametric type II radio bursts // Astron. Lett. V. 33. N 3. P. 192–202. 2007. https://doi.org/10.1134/S1063773707030061
– *Chernov G.P.* Manifestation of quasilinear diffusion on whistlers in the fine structure radio sources of solar radio bursts // Plasma Phys. Rep. V. 31. N 4. P. 314–324. 2005. https://doi.org/10.1134/1.1904148
– *Chernov G.P.* Unusual stripes in emission and absorption in solar radio bursts: Ropes of fibers in the meter wave band // Astron. Lett . V. 34. N 7. P. 486–499. 2008. https://doi.org/10.1134/S1063773708070074
– *Chernov G.P.* Fine structure of solar radio bursts. Heidelberg: Springer, 282 p. 2011. https://doi.org/10.10007/978-3-642-20015-1
– *Chernov G.P.* Latest data on the fine structure in solar radio emission / LAMBERT Academic Publisher. Riga, Latvia, 284 p. 2019.
– *Chernov G.P., Fomichev V.V., Sych R.A.* A model of zebra patterns in solar radio emission // Geomagn. Aeronomy. V. 58. N 3. P. 394–406. 2018. https://doi.org/10.1134/S0016793218030040
– *Elgarøy Ø.* Observations of the fine structure of enhanced solar radio radiation with a narrow-band spectrum analyser // Nature . V. 184. N 4690. P. 887–888. 1959. https://doi.org/10.1038/184887a0
– *Fomichev V.V., Fainstein S.M., Chernov G.P.* A possible interpretation of the zebra pattern in solar radiation // Plasma Phys. Rep. V. 35. N 12. P. 1032–1035. 2009. https://doi.org/10.1134/S1063780X09120058
– *Karlický M., Bárta M., Jiřička K., Meszárosová H., Sawant H.S., Fernandes F. C.R., Cecatto J.R.* Radio bursts with rapid frequency variations – lace bursts // Astron. Astrophys. V . 375. N 2. P. 638–642. 2001. https://doi.org/10.1051/0004-6361:20010888
– *Karlický M.* Radio continua modulated by waves: Zebra patterns in solar and pulsar radio spectra // Astron. Astrophys. V. 552. ID A90. 2013. https://doi.org/10.1051/0004-6361/201321356
– *Karlický M* . Frequency variations of solar radio zebras and their power-law spectra // Astron. Astrophys . V. 561. ID A34. 2014. https://doi.org/10.1051/00046361/201322547
– *Karlický M.* Simulations of the solar radio zebra // Astron. Astrophys. V. 661. ID A56. 2022. https://doi.org/10.1051/0004-6361/202142497
– *Kuijpers J.* Collective wave-particle interactions in solar type IV radio sources. Ph.D. Thesis. Utrecht, The Netherlands: Utrecht University. 72 p. 1975.

– *Kuijpers J.* Theory of type IV dm Bursts // Symposium - International Astronomical Union. V. 86. P. 341–361. 1980. https://doi.org/10.1017/S0074180900037098
– *Kuznetsov A.A., Tsap Yu.T.* Loss-cone instability and formation of zebra patterns in type IV solar radio bursts // Sol. Phys. V. 241. P. 127–148. 2007. https://doi.org/ 10.1007/S11207-006-0351-7
– *LaBelle J., Treumann R.A., Yoon P.H., Karlický M.* A model of zebra emission in solar type IV radio bursts // Astrophys. J. V. 593. N 2. P. 1195–11207. 2003. https://doi.org/10.1086/376732.
– *Laptuhov A.I., Chernov G.P.* New mechanism for the formation of discrete stripes in the solar radio spectrum // Plasma Phys. Rep . V. 32. N 10. P. 866–871. 2006. https://doi.org/10.1134/S1063780X06100060
– *Laptuhov A.I., Chernov G.P.* Concerning mechanisms for the zebra pattern formation in the solar radio emission // Plasma Phys. Rep. V. 35. N 2. P. 160–168. 2009. https://doi.org/10.1134/S1063780X09020081
– *Litvinenko G.V., Shaposhnikov V.E., Konovalenko A.A., Zakharenko V.V., Panchenko M., Dorovsky V.V., Brazhenko A.I., Rucker H.O., Vinogradov V.V., Melnik V.N.* Quasi-similar decameter emission features appearing in the solar and jovian dynamic spectra // Icarus. V. 272. P. 80–87. 2016. https://doi.org/10.1016/j.icarus.2016.02.039
– *Mollwo L.* Interpretation of patterns of drifting zebra stripes // Sol. Phys. V. 83. N 2. P. 305–320. 1983. https://doi.org/10.1007/BF00157482
– *Mollwo L.* The magneto-hydrostatic field in the region of Zebra patterns in solar type-IV dm-bursts // Sol. Phys. V. 116. N 2. P. 323–348. 1988. https://doi.org/10.1007/BF00157482
– *Panchenko M, Rošker S., Rucker H.O. et al.* Zebra pattern in decametric radio emission of Jupiter // Astron. Astrophys. V. 610. ID A69. 2018. https://doi.org/10.1051/0004-6361/201731369
– *Selhorst C.L., Silva-Válio A., Costa J.E.R* . Solar atmospheric model over a highly polarized 17 GHz active region // Astron. Astrophys . V. 488. N 3. P. 1079–1084. 2008. https://doi.org/ 10.1051/0004-6361:20079217
– *Slottje C* . Peculiar absorption and emission microstructures in the type IV solar radio outburst of March 2, 1970 // Sol. Phys. V. 25. N 1. P. 210–231. 1972. https://doi.org/10.1007/BF00155758
– *Slottje C.* Atlas of fine structures of dynamics spectra of solar type IV-dm and some type II radio bursts. Utrecht, The Netherlands: Dwingeloo Observatory, 233 p. 1981.
– *Treumann R.A., Gudel M., Benz A.O* . Alfven wave solitons and solar intermediate drift bursts // Astron. Astrophys. V. 236. N 1. P. 242–249. 1990.

– *Viktorov M., Mansfeld D., Golubev S* . Laboratory study of kinetic instabilities in a nonequilibrium mirror-confined plasma // Europhys. Lett. V. 109. N 6. ID 65002. 2015. https://doi.org/10.1209/0295-5075/109/65002

– *Winglee R.M. and Dulk G.A.* The electron-cyclotron maser instability as a source of plasma emission // Astrophys. J. V. 307. P. 808–819. 1986. https://doi.org/10.1086/164467

– *Yasnov L.V., Chernov G.P.* Alternative models of zebra patterns in the event on June 21, 2011 // Sol. Phys. V. 295. N 2. ID 13. 2020. https://doi.org/10.1007/s11207-020-1585-5

– *Yasnov L.V., Karlický M., Stupishin A.G.* Physical conditions in the source region of a zebra structure // Sol. Phys. V. 291. N 7. P. 2037–2047. 2016. https://doi.org/10.1007/s11207-016-0952-8

– *Yasnov L.V., Karlický M* . M agnetic field, electron density and their spatial scales in zebra pattern radio sources // Sol. Phys. V. 295. N 7. ID 96 . 2020. https://doi.org/ 10.1007/s11207-020-01652-w

– *Zheleznyakov V.V., Zlotnik E.Ya* . Cyclotron wave instability in the corona and origin of solar radio emission with fine structure // Sol. Phys. V. 43. N 2. P. 431–451. 1975a. https://doi.org/10.1007/BF00152366

– *Zheleznyakov V.V., Zlotnik E.Ya.* Cyclotron wave instability in the corona and origin of solar radio emission with fine structure. III. Origin of zebra pattern // Sol. Phys. V. 44. N 2. P. 461–470. 1975b. https://doi.org/10.1007/BF00153225

– *Zheleznyakov V.V., Zlotnik E.Ya., Zaitsev V.V., Shaposhnikov V.E* . Double plasma resonance and its manifestations in radio astronomy // Phys.-Usp. V. 59. N 10. P. 997–1120. 2016. https://doi.org/10.3367/UFNe.2016.05.037813

– *Zlotnik E.Ya., Zaitsev V.V., Aurass H., Mann G., Hofmann A.* Solar type IV burst spectral fine structures. II. Source model // Astron. Astrophys. V. 410. N 3. P. 1011–1022. 2003. https://doi.org/10.1051/0004-6361:20031250

– *Zlonik E.Ya., Zaitsev V.V., Aurass H., Mann G.A* . Special radio spectral fine structure used for plasma diagnostics in coronal magnetic traps // Sol. Phys. V. 255. N 2. P. 273–288. 2009. https://doi.org/10.1007/s11207-009-9327-8

– *Zlotnik E.Y., Shaposhnikov V.E., Zaitsev V.V.* Interpretation of the zebra pattern in the Jovian kilometric radiation // J. Geophys. Res. – Space. V. 121. N 6. P. 5307–5318. 2016. https://doi.org/10.1002/2016JA022655

FIGURE CAPTIONS

Fig. 1. Complex zebra structure according to the IZMIRAN spectrograph data in the range of 180-270 MHz in the event of 18.07.2000.

Fig. 2. Complex event of 01.12.2004 with a smooth transition of fiber bursts into zebra structure stripes with a sawtooth frequency drift in the range of 1.1-1.34 GHz (Huairou station, National Astronomical Observatory of China (NAOC)) in the event of 01.12.2004.

Fig. 3. (*a*) Harmonics of the cyclotron frequency $s\,\omega_{Be}$ and plasma frequency ω_{Pe} as functions of the coordinate x for characteristic scales of magnetic field variation LB and density LN at $|LB| < |LN|$ (fragment of Fig. 2 from [Zheleznyakov et al., 2016]);

(*b*) Profile of electron density as a function of height h in the solar atmosphere according to [Selhorst et al. , 2008]).

Fig. 4. Height dependence of plasma frequency in accordance with the barometric law (bold line) and height profiles of electron cyclotron harmonics s (thin lines) in the solar corona. For electron temperature $T_e = 1.2 \cdot 10^6$ K and initial frequency $f_{P0} = 3800$ MHz at height $h_{B0} = 20{,}000$ km, 34 DPR levels are formed in the corona between plasma levels of 2600-3800 MHz (from [Laptuhov and Chernov, 2009]).

Fig. 5. Dynamic plasma emission spectrum. The types of kinetic instabilities considered in the work are highlighted: 1) initial stage of ECR discharge (rarefied plasma); 2 and 3) developed discharge stages (dense plasma); 4) initial phase of plasma decay (dense plasma); 5) decaying plasma (rarefied plasma). Three lines on the spectrogram show the time variation of corresponding frequencies $2f_{ce0}$, f_{ce0} and $1/2f_{ce0}$, where $f_{ce0} \equiv f_{ce}$ − electron cyclotron frequency at the center of the magnetic trap on its axis. E electron cyclotron frequency at the center of the magnetic trap on its axis ECR heating switch-off.

(fragment of Fig. 2 from [Viktorov et al., 2015]) . Note the strict periodicity of whistler generation.

Fig. 6. Example of ZS in Jupiter's radio emission observed at the Ukrainian radio telescope URAN-2, January 30, 2014. Fragment of Fig. 1 from [Panchenko et al., 2018].

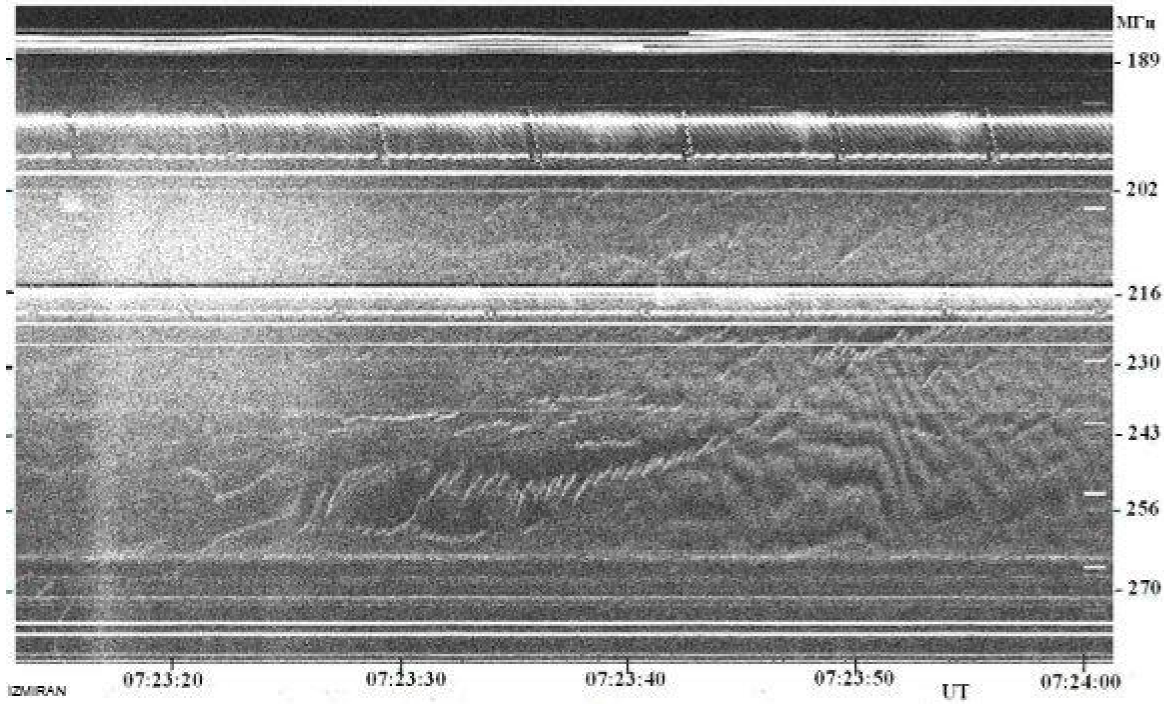
МГц
189
202
216
230
243
256
270
IZMIRAN
07:23:20
07:23:30
07:23:40
07:23:50
UT
07:24:00

Fig. 1.

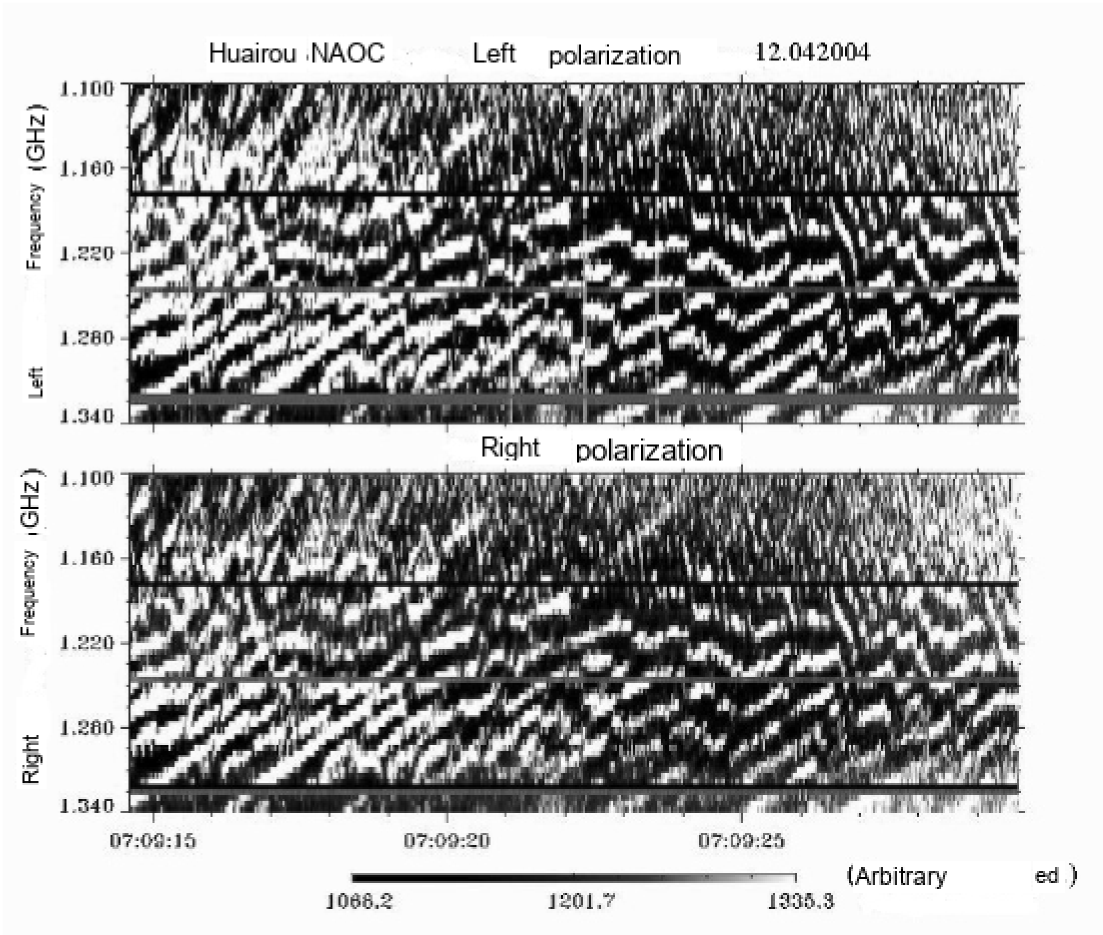
Huairou NAOC
Left polarization
12.042004
Frequency (GHz)
Left
1.100
1.160
1.220
1.280
1.340
Right polarization
Frequency (GHz)
Right
1.100
1.160
1.220
1.280
1.340
07:09:15
07:09:20
07:09:25
(Arbitrary ed)
1066.2
1201.7
1335.3

Fig. 2.

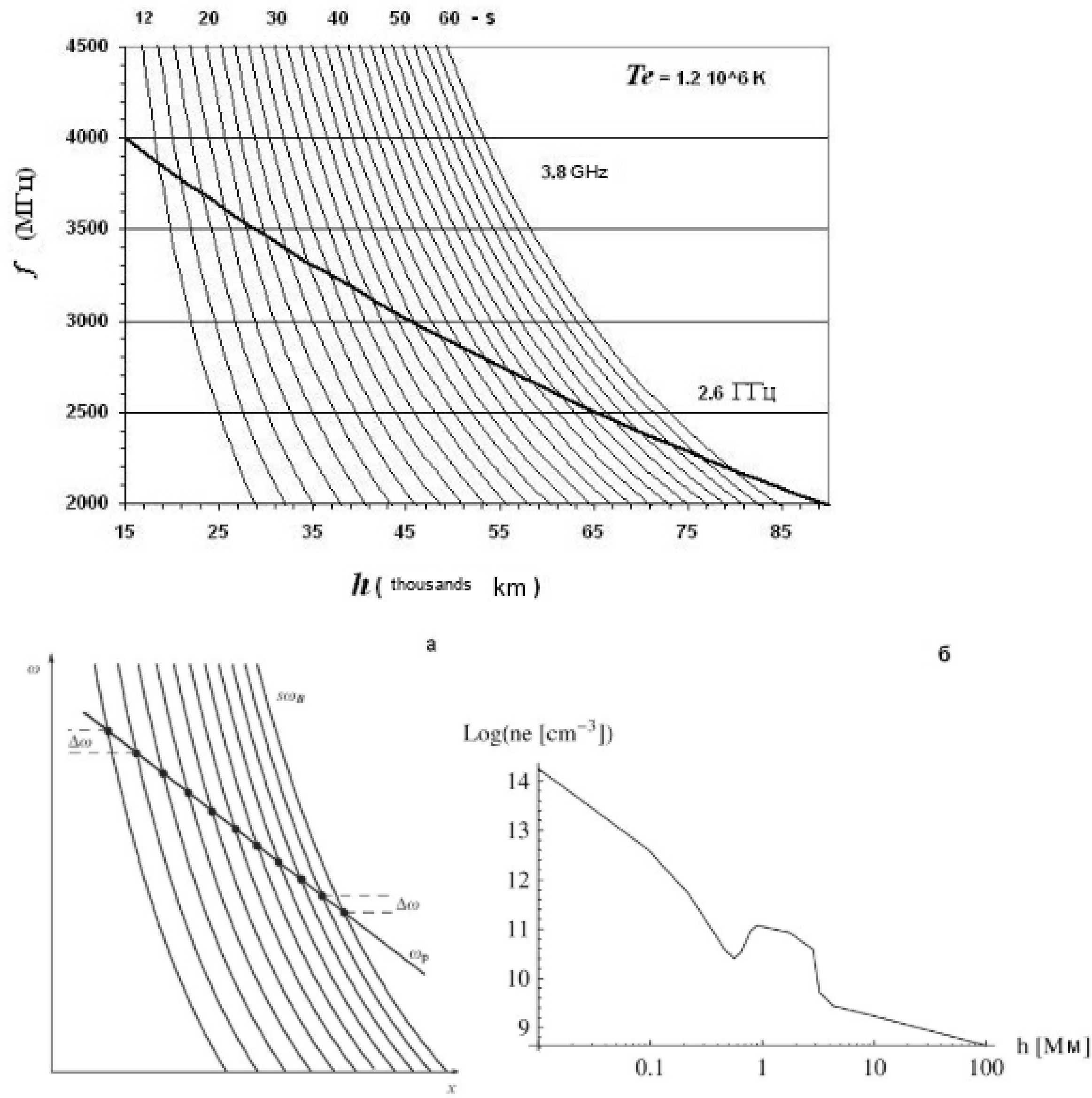

12 20 30 40 50 60 - s
Te = 1.2 10^6 K
f (МГц)
3.8 GHz
2.6 ГГц
4500
4000
3500
3000
2500
2000
15 25 35 45 55 65 75 85
h (thousands km)
а
б
ω
$s\omega_B$
Δω
Δω
ω_p
x
Log(ne [cm^-3])
14
13
12
11
10
9
0.1 1 10 100
h [Мм]

Fig. 3.

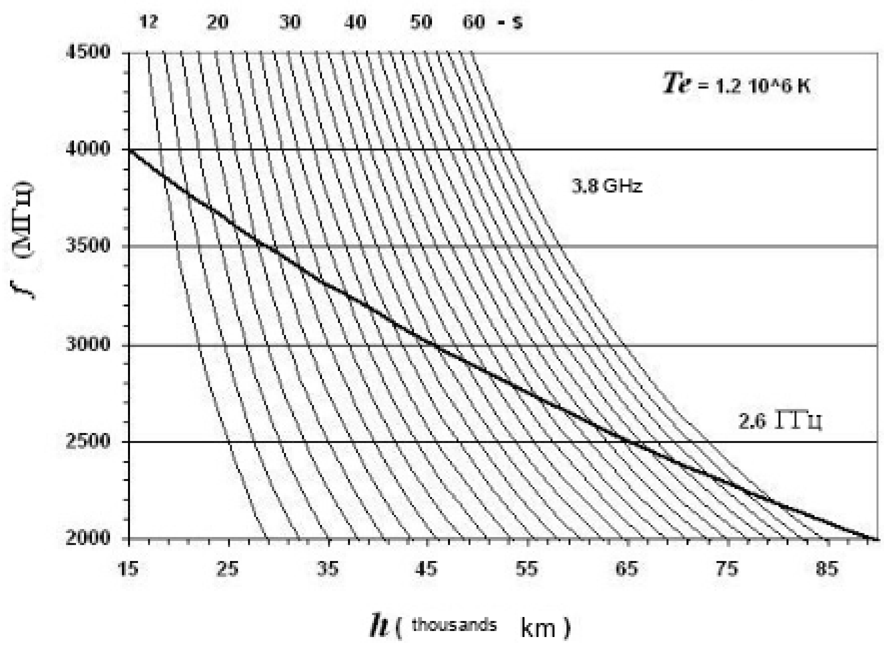

12 20 30 40 50 60 - s
4500
4000
3500
3000
2500
2000
f (МГц)
Te = 1.2 10^6 K
3.8 GHz
2.6 ГГц
15 25 35 45 55 65 75 85
h (thousands km)

Fig. 4.

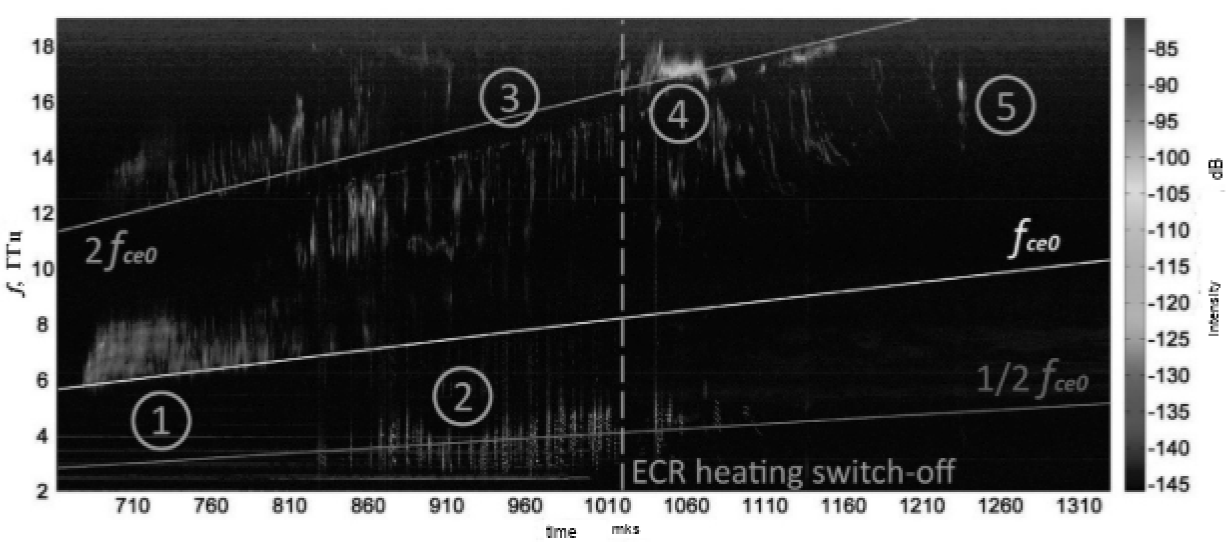

18
16
14
12
10
8
6
4
2
f, ГГц
3
4
5
2 fce0
fce0
1
2
1/2 fce0
ECR heating switch-off
710 760 810 860 910 960 1010 1060 1110 1160 1210 1260 1310
time mks
-85 -90 -95 -100 -105 -110 -115 -120 -125 -130 -135 -140 -145
dB
Intensity

Fig. 5.

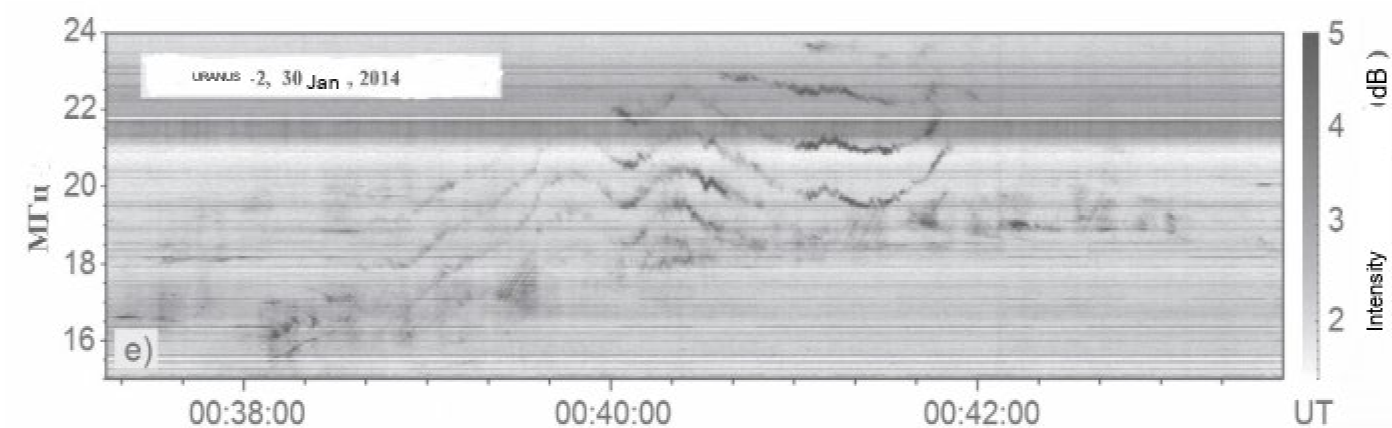

URANUS -2, 30 Jan , 2014
24
22
20
18
16
MГц
e)
00:38:00
00:40:00
00:42:00
UT
5
4
3
2
Intensity
(dB)

Fig. 6.